Spatial and temporal variation of seismic *b*-values across the West Tehran

Mehrzad Azizi · Hamid Saffari

Abstract Until now, numerous efforts have been made to find earthquake precursors. One of the factors that can predict the occurrence of future earthquakes is a decrease in the *b-value* parameter. In this study, for the metropolis of Tehran, with a population of over 8 million, located on or near many active faults, it is estimated that if the maximum seismic potential of these faults happened again, the greatest disaster in human history would occur. In this case, the analyses indicate a minimum of several hundred thousand casualties and sometimes more than a million. In the current study, various faults around Tehran were investigated, and given that the faults on Tehran have not had serious seismic activity for over a thousand years, this article focused exclusively on adjacent faults, particularly the Eshtehard faults. Therefore, in the current study, the seismicity and tectonics of western Tehran were investigated by analyzing seismic parameters using earthquake data collected from 2003 to 2023. In general, the investigation of the temporal changes in the study area showed that the *b-value* decreased before the December 20, 2017, earthquake and an increasing trend afterward. Observing anomalies in the *b-value* before and after the main movement in the area shows that changes in this parameter can be considered a precursor for estimating the time and location of earthquakes. Therefore, a useful step can be taken toward knowing the local seismic hazards by using earthquake data recorded by seismic networks and continuously monitoring the changes in the *b-value*.

Keywords Earthquake forecast · *b-value* · Eshtehard fault · Seismicity · Seismic network

1 Introduction

The forecast of the future large earthquakes is a vital issue that remains uncertain despite significant advances in science and technology. Tehran, the current capital of Iran, with a population of over 8 million people, located in the Central Alborz Range, has become the country's largest center of human and economic concentration. Due to the presence of active fault systems around the Tehran region, several studies have been conducted to analyze the seismicity of this metropolis. In the event of a severe earthquake in these faults, high-rise structures in Tehran, especially those that do not have a suitable lateral restraint system based on seismic codes, will be seriously damaged. In Tehran, more than a thousand tall buildings have a long period and are affected by distant

M. Azizi
Shahid Beheshti University, Tehran, Iran
e-mail: meh.azizi@mail.sbu.ac.ir

H. Saffari (✉)
Department of Structure & Earthquake, Faculty of Civil, Water & Environmental Engineering, Shahid Beheshti University, Tehran, Iran
e-mail: h_saffari@sbu.ac.ir

earthquakes. They need to be designed to withstand severe earthquakes away from faults. Therefore, due to the area's seismicity, the presence of multiple faults, and the threats resulting from them, which could cause significant financial and human losses in the metropolis of Tehran, it is essential to analyze the seismicity of Tehran and provide crisis management solutions to prevent disasters. Therefore, this study has been chosen to investigate the seismicity of the west of Tehran using seismic parameters.

Nowadays, *b-value*, *a-value*, and fractal analysis are widely used in seismic studies. The Gutenberg-Richter relationship is the most practical model proposed to explain a region's variation of seismicity characteristics. The Gutenberg-Richter relationship, which shows the number of earthquake occurrences in a region as a function of magnitude, can be expressed in a simple form as the following equation:

$$LogN = a - bM \tag{1}$$

In this equation, N is the number of earthquake occurrences with magnitudes greater or equal to M, and a and b are parameters that can be different depending on the region under investigation. Two parameters, a and b, are known as seismic parameters. The parameter of a represents the seismicity level of the region, and the higher its value, the higher the probability of seismicity in that region. The *a*-value depends on factors such as the area of the study, the seismicity rate, the size of the seismic sources, and the time span of years for which the data are calculated (Gutenberg & Richter 1944). The parameter b is the slope of the frequency-magnitude diagram (FMD), whose value varies in different regions and is usually between 0.4 and 1.8 for different tectonic regions (Miyamura 1962). The b parameter is related to the tectonic features of the region, so that its changes can indicate the structural heterogeneity or epicentral distribution of earthquakes in the region. The high values of b indicate a higher ratio of small earthquakes to large ones. According to Bayrak et al. (2002), the smaller the value of b is, the higher the ratio of large earthquakes to small ones, and vice versa. Additionally, as Wyss (1973) stated, there is an inverse relationship between the value of b and the level of accumulated stress in a region. Therefore, low values of b are associated with high heterogeneity, greater stress accumulation, high strain rate, and the presence of major faults (Manakou & Tsapanos 2000).

The methods commonly used to calculate the b parameter include the maximum likelihood method (MLE) (Aki 1965; Shi & Bolt 1982; Utsu 1965) and the least squares method (LSM) (Main 2000; Zöller et al. 2002). The maximum likelihood method considers an equal contribution from each seismic event and calculates the magnitude of all earthquakes with equal weight as an average. Compared to the maximum likelihood method, the least squares method considers a higher weight for small and medium earthquakes (Xie et al. 2022). Based on previous studies (Goldstein et al. 2004; Nava et al. 2017; Newman 2005; Bengoubou-Valerius and Gibert 2013), the standard deviation of the least squares method is more than twice that of the maximum likelihood method. For catalogs of small earthquakes, the maximum likelihood method provides a more accurate estimate than the least squares method. In this study, we use a maximum likelihood estimate to estimate the b- and a-values and their confidence limits. The b parameter in Eq. 1 can be estimated using Eq. 2 (Aki 1965; Bender 1983; Utsu 1965):

$$\widehat{b} = \frac{1}{\overline{M} - M_{min}} loge \tag{2}$$

where $\overline{M}$ refers to the average magnitude of earthquakes in the earthquake catalog, and M_{min} is the minimum magnitude. The standard deviation of the b parameter can be calculated using formula 3 (Shi and Bolt 1982):

$$\delta b = 2.3 b^2 \sqrt{\frac{\sum_{i=1}^{n} \left(M_i - \overline{M} \right)^2}{n(n-1)}} \tag{3}$$

where n is the total number of earthquakes that occurred in the region, $\overline{M}$ is the average magnitude of earthquakes in the catalog, and M_i is the magnitude of the ith earthquake. The zmap7 software (Wiemer 2001; Wiemer and Wyss 2000) was used for earthquake data analysis.

The fractal dimension is another concept that helps us in seismology and the tectonic earthquake of a region. The fractal dimension is used to estimate the fractal dimension of the spatial and temporal distribution of earthquakes (Kagan & Knopoff 1980). As we know, most earthquakes occur due to the activation of faults and the resulting fractures. Kagan (1993) states

that earthquakes do not occur on a uniform surface but rather on multiple faults that are close to each other and have a fractal-like structure. Based on this, earthquakes can be represented with a self-similar mathematical structure. The fractal dimension parameter defined in such a self-similar mathematical structure is the earthquake fractal dimension.

The correlation integral method was used to calculate the fractal dimension of earthquake epicenters. According to this method, the correlation dimension of the spatial distribution of earthquake activity in a region is given by Grassberger and Procaccia (1983):

$$D = \frac{Lim \, log \, C(r)}{log \, r} r \to 0, \tag{4}$$

where $C(r)$ is the correlation function, which is given by

$$C(r) = \frac{2}{N(N-1)} N(R < r) \tag{5}$$

In this equation, $N(R < r)$ is the number of pairs of earthquakes (Xi, Xj) with separation less than r. If the distribution of earthquake epicenters has a fractal structure, the relationship:

$$C(r) \propto r^D \tag{6}$$

where D is the fractal or correlation dimension.

## 2 Tectonic and seismic position

Due to Iran's location in the Alp-Himalaya, the seismic belt is formed by multiple tectonic plates, each with different seismic characteristics. The Alborz region in northern Iran has a width of 60 to 120 km and approximately includes the Alborz area and the southern coast of the Caspian Sea (Fig. 1a). This region has experienced severe seismic activity throughout history (Priestly et al. 1994). The major faults in this region have a reverse slip component along the northeast-southwest direction, and their activity has caused various geological formations to be displaced against each other, as well as the emergence of uplifted plateaus in the region. The occurrence of destructive earthquakes in the Alborz region, the southern Caspian Sea basin, and the northern part of central Iran indicates strong tectonic activities. The current movements in the Alborz region are related to

a series of tectonic events resulting from the collision of Eurasia with central Iran and Eurasia with Arabia (Allen et al. 2003). Recent GPS measurements have shown that the intracontinental deformation resulting from the convergence of the Eurasian-Arabian plates continues in an NNE direction at a slip rate of 22 mm per year. The Global Positioning System (GPS) ((Fig. 1a, b) indicates a shortening of the NNE direction in the Alborz region at a rate of 5 ± 2 mm per year and a left-lateral motion at a rate of 4 ± 2 mm per year (Rashidi & Derakhshani 2022). Investigations of the tectonic structures in the Alborz region, as well as the analyses and measurements conducted in this area, have shown that the most important structural elements in the region are the low-angle thrust faults and associated fold structures. The displacements along these faults have significantly impacted the formation and shortening of the Alborz range.

3 Data and methodology

This study investigated the western part of Tehran at longitude 49.324 to 51.051° and latitude 35.39 to 35.98° (Fig. 2). The data utilized in this research were obtained from the national seismic database of the Institute of Geophysics at the University of Tehran, covering the period from 2003 to 2023. This dataset includes 185 seismic events with magnitudes ranging from 2.5 to 5.2 within the study area.

According to Wiemer and Wyss (2000), to calculate the seismicity parameters a and b, it is necessary to calculate the complete magnitude and use a homogeneous database. For each region, there exists a magnitude that, based on neighboring seismic stations and networks, can record all seismic events in the region. This magnitude is called the "magnitude of completeness" (M_C), and according to its definition, all earthquakes in the region are recorded as the smallest magnitude, as stated by Wiemer and Wyss (2002). The M_C is an important parameter in earthquake hazard assessment, as it represents the minimum magnitude that seismic instruments in the region can record. Using the M_C value and a homogeneous earthquake database, seismicity parameters a and b can be calculated. These parameters are critical in determining earthquake risk and designing earthquake-resistant structures.
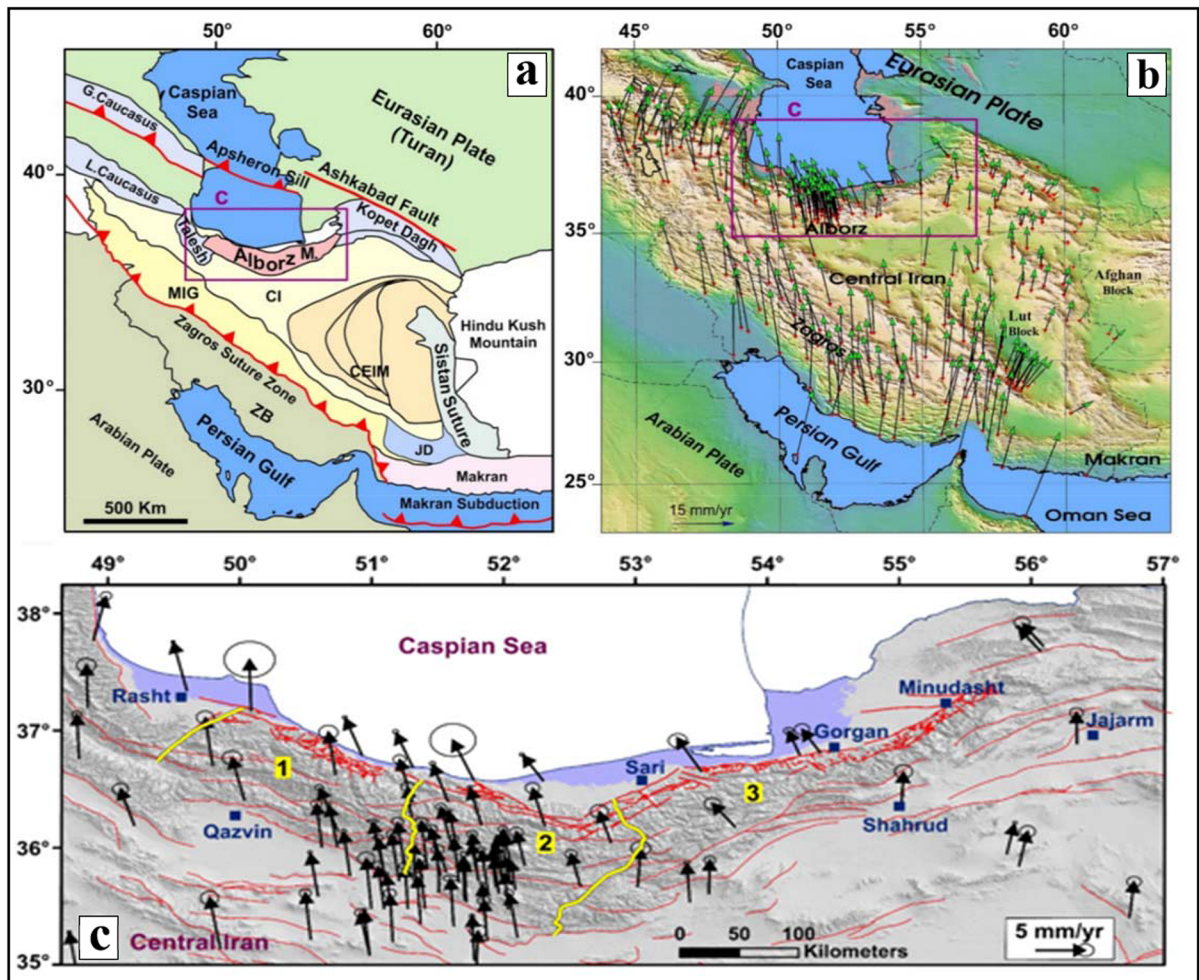
Fig. 1 **a** Tectonic structure of the Arabian-Eurasian collision zone and the location of the studied subdomains (Alborz; purple rectangle) (ZB, Zagros belt; MIG, magmatic and metamorphic inner-Iranian zone; CEIM, Central-Eastern Iranian Micro-continent; CI, Central Iran; and JD, Jazmurian depression). **b** GPS velocity field with respect to the Eurasian reference frame. **c** GPS velocity field in the rectangular area (Rashidi and Derakhshani 2022)

Therefore, determining the M_C for each region is an essential step in earthquake hazard assessment and seismic monitoring. Various methods are available to calculate the M_C and one of these methods is the maximum curvature method proposed by Wiemer and Wyss (2000). This method can estimate the complete magnitude of data that follows the Gutenberg-Richter law. Based on the maximum curvature method, a frequency-magnitude plot was generated for seismic events in the study region during the period of December 2003 to January 2023 to estimate the magnitude of completeness. The maximum curvature point on the plot corresponds

to the magnitude of completeness, below which the frequency-magnitude distribution is no longer complete. The resulting frequency-magnitude plot showed that the complete magnitude for the study region was 2.5, as indicated in Fig. 3.

In the frequency-magnitude distribution plot, the red line indicates the best fit for the calculated network data. The slope of the red line represents the *b-value*, and the intercept from the origin indicates the *a-value* of the Gutenberg-Richter relationship.
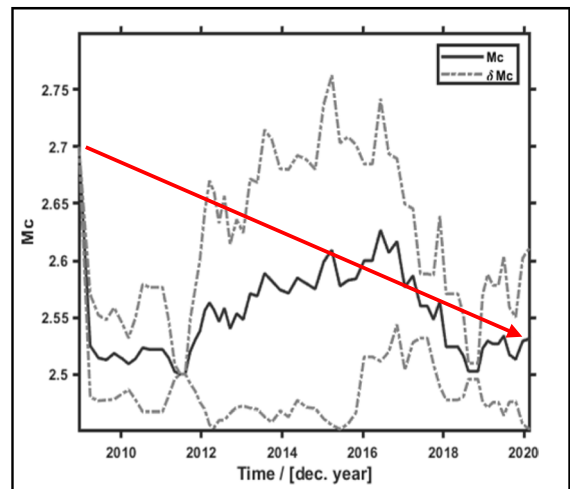
To obtain a more accurate assessment of the M_C over time, we investigated and determined the temporal changes in the data's completeness magnitude
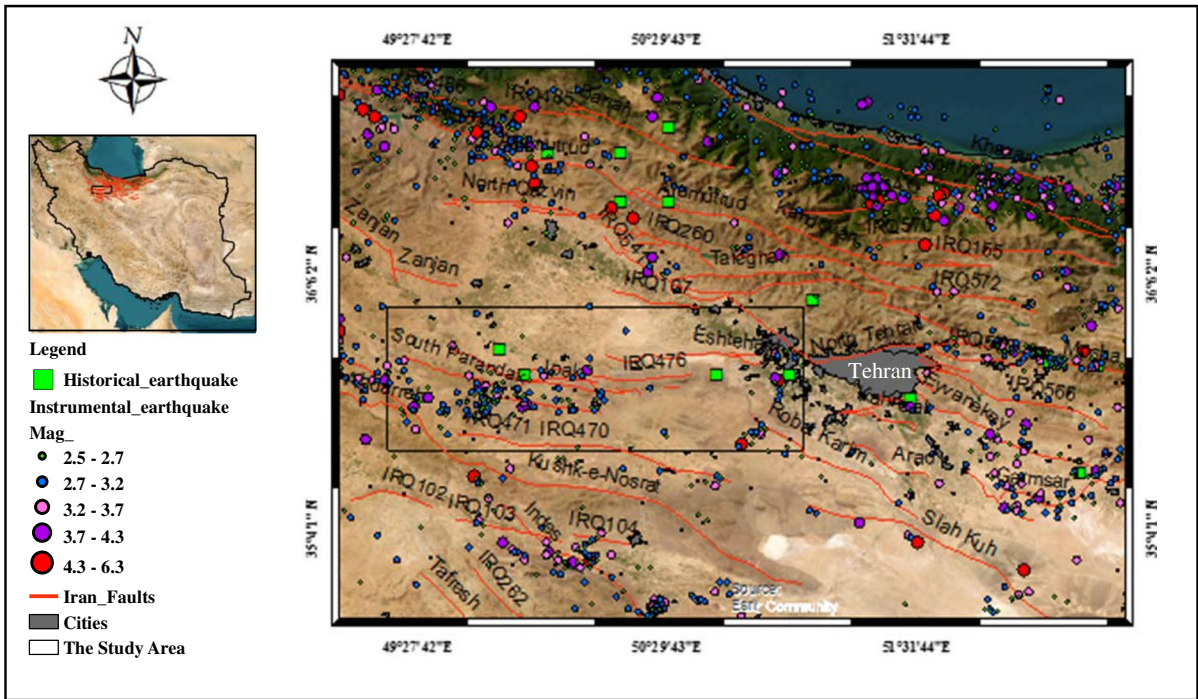
Fig. 2 Distribution of historical and instrumental earthquake epicenters
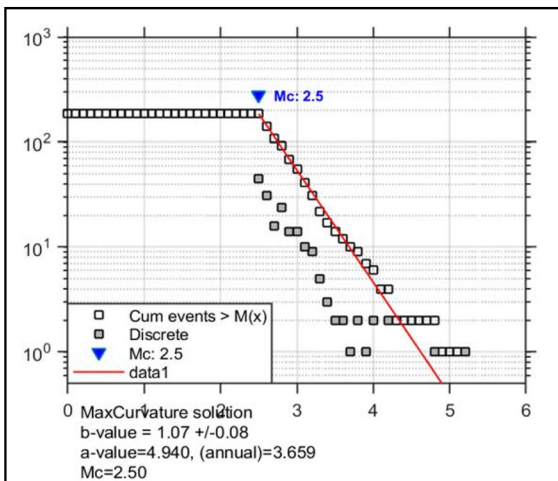
Fig. 3 The frequency-magnitude plot for the seismic events in the study region during the period of December 2003 to January 2023

Fig. 4 Temporal changes and decreasing trend (arrow direction) of the completeness magnitude (M_C) of the data set in the study range during the period of December 2003 to January 2023

(M_C) using an overlapping moving window (window overlap 4%). In this method, a moving window of 50 events with 5 event increments is used to calculate the temporal variation of M_C. As shown in Fig. 4, the

M_C variations increase from approximately 2.7 at the beginning of the study period to around 2.53 in the final years of the period.

As can be seen, the overall trend of the seismicity changes in the study area indicates a decreasing trend of completeness magnitude (M_C) over time. This indicates an improvement in the performance of seismographic networks in recording earthquakes in the study area.

(Figure 5a and b show the cumulative frequency-magnitude distribution plot in terms of the number of earthquakes and the number per year, respectively. From 2003 to 2023 (Fig. 5a), we observe a relatively rapid decrease in the frequency of events up to a magnitude of about 3.4. After that, a nearly constant slope

is observed in the number of events up to magnitude 4. These plots represent the behavior of earthquake occurrences during the study period in the specified region.

The cumulative chart of depth changes to the number of events (Fig. 6a, b) shows the depth of earthquakes in this region up to 28.7 km. It is important to note that seismic stations cannot accurately measure the depth of earthquakes, and the region's tectonics and the depth of earthquakes should be considered to verify the depth of the events.
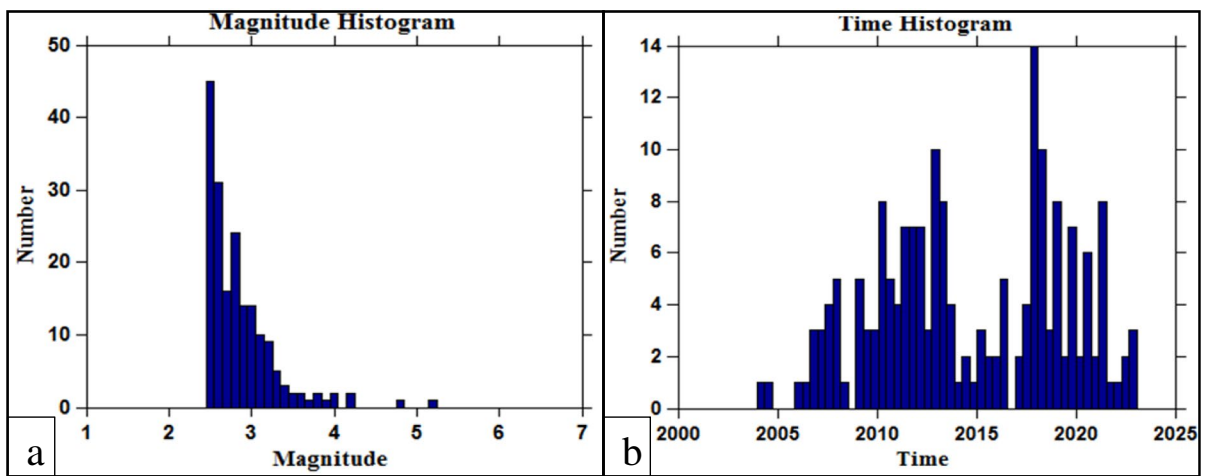
Fig. 5 a Cumulative distribution plot of earthquake magnitude by count. **b** Number of earthquakes per year plot
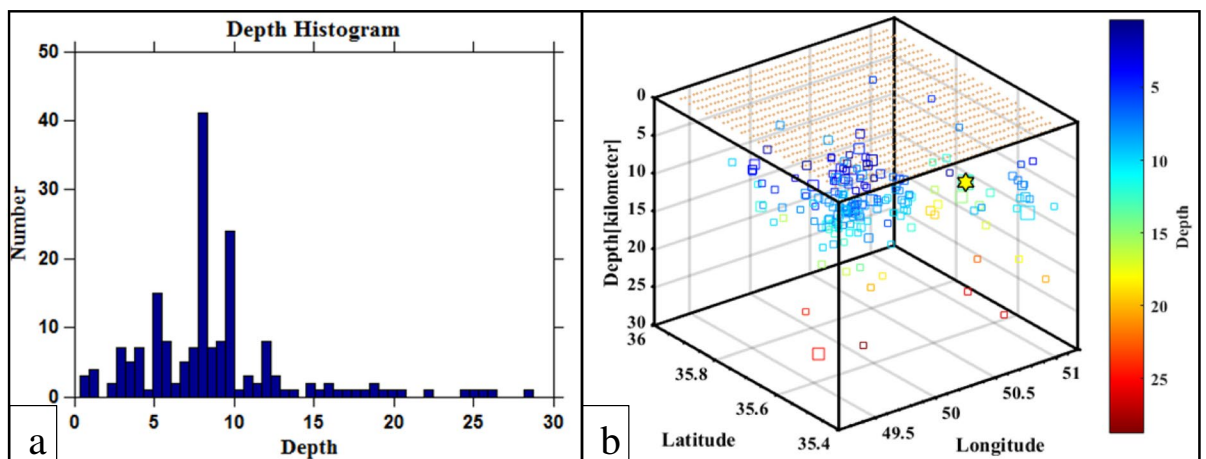
Fig. 6 a, **b** Cumulative graph of depth changes in relation to the number of events. The yellow star represents the epicenter location of the 20 December 2017 (Mw 5.2) Malard earthquake

The magnitude-time plot of earthquakes is a helpful indicator for identifying the seismicity level of the region. Figure 7 shows that most regional earthquakes have magnitudes less than 5. However, this region has experienced numerous destructive earthquakes throughout history, causing significant casualties. We can mention the historical earthquakes of 7.2 in 2000 AD and 20/12/2017 in Malard, which can be seen in the picture below.

Figure 8 shows the pattern of migration of seismic centers before and after the 5.2 magnitude earthquake in Malard. As seen in the figure, the direction of seismic displacements indicates a north–south distribution and does not show a direct correlation with the seismotectonic activity of the Eshtehard fault zone. According to the studies of Mehrnia (2017), the distribution of earthquakes in the east of Alborz province follows spiral shapes, and a number of seismic events have a significant geometric relationship with the main epicenter of Malard. The spiral of the Malard earthquake has spread to the west (north-southwest direction) and parallel to the meridians. The possibility of increasing aftershocks in the eastern part of the Malard spiral is much less than in the west. This means that Malard earthquakes do not have a significant geometrical effect on the North Tehran fault. However, the authors suggest that since the release

of stress from this block could potentially propagate stress to adjacent blocks, such as the northwestern block (the North Tehran fault), an increase in seismicity in neighboring blocks should be monitored. By analyzing seismic parameters, predictions can be made about the occurrence of more severe events in the future near the metropolitan areas of Tehran and Karaj. The order of occurrence of earthquakes is shown in Table 1.

4 Results and discussion

4.1 Spatial distribution of the b-value

The *b*-value map provides valuable information about the tectonics of the studied region. In order to investigate spatial changes in stress in the study area, maps of *b*-value and *a*-value were drawn using the maximum likelihood estimation method. The spatial variation of the *b*-value was obtained using 185 seismic events recorded between 2003 and 2023 and we used the ZMap7 software program. To draw the spatial distribution map, meshing in the dimensions of $0.05 \times 0.05°$ is designed to estimate each node's value of parameter *b* using the maximum likelihood method. Figure 9 shows the spatial variations of the

**Fig. 7** Bar graph of the magnitude of earthquakes by year
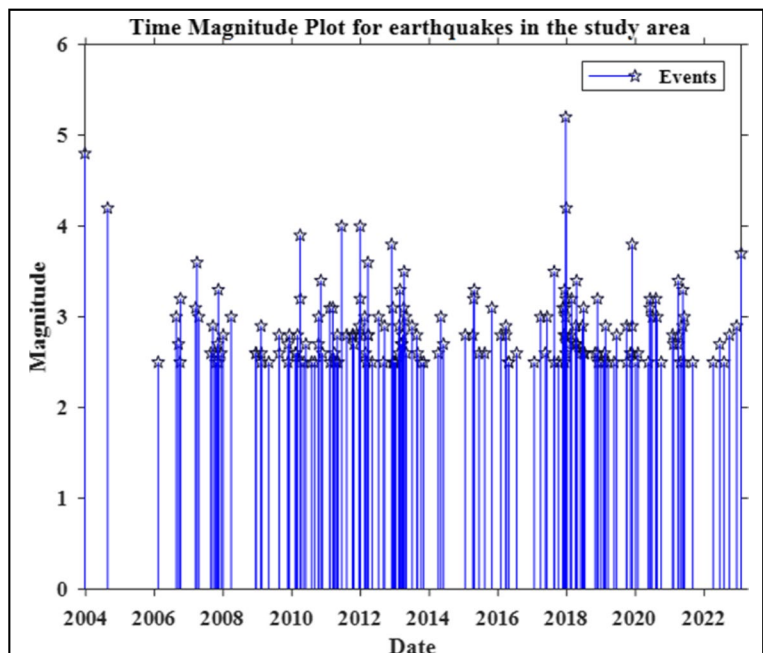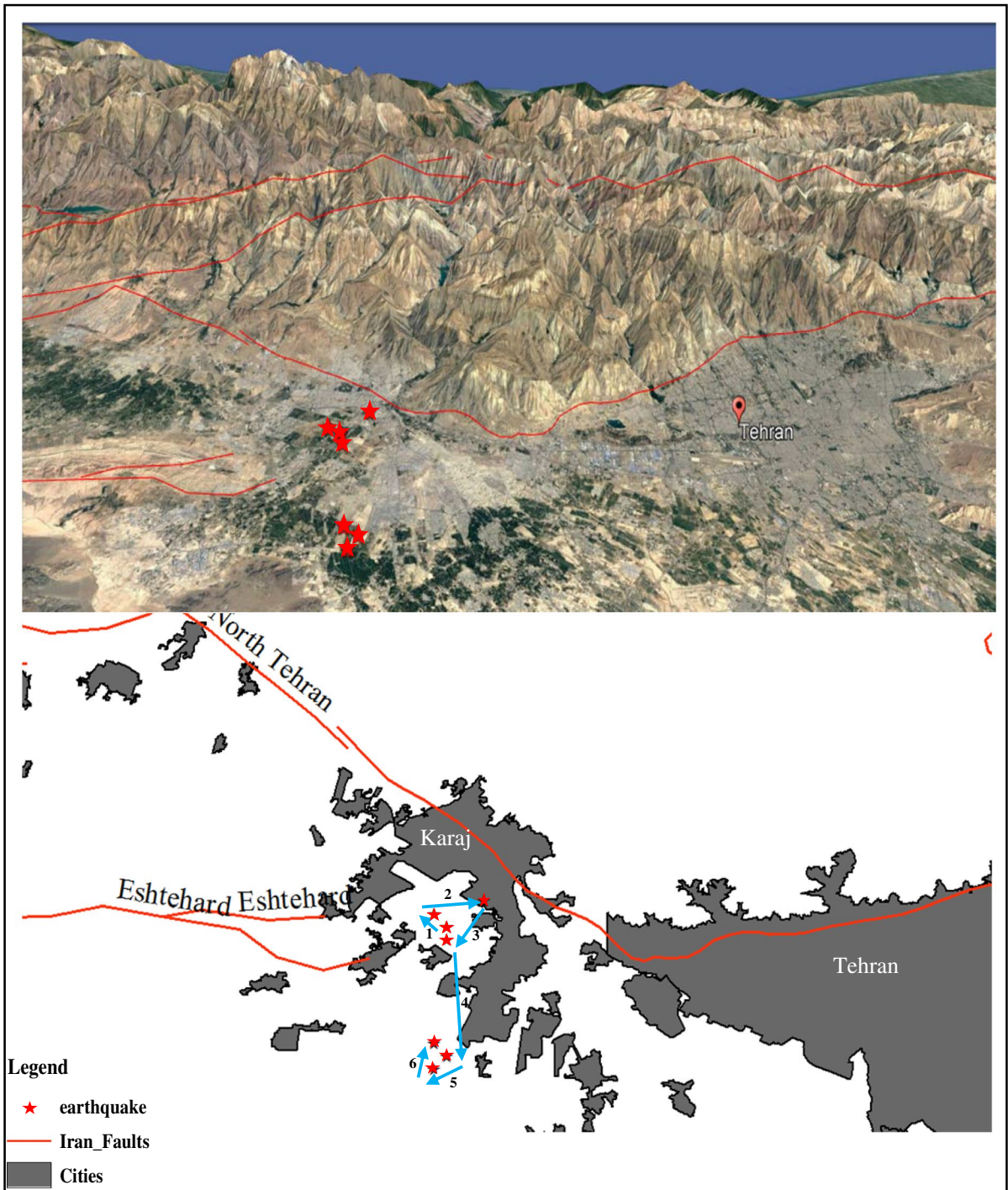
Fig. 8 The pattern of migration of seismic centers in the Eshtehard fault zone. The blue arrows show the migration pattern of seismic centers before and after the 5.2 Malard earthquake

Table 1 Migration of aftershoks according to the time of occurrence

No	Event ID	Origin time	Lat	Long	Depth (km)	Mag
1	128008	2017/12/02 23:41:06.5	35.77	50.945	16	2.8
2	128635	2017/12/09 13:03:50.5	35.776	50.944	19	3.3
3	128715	2017/12/10 07:25:35.6	35.792	50.977	13	2.5
4	128981	2017/12/12 19:48:54.8	35.763	50.951	17.7	3.1
5	129954	2017/12/20 19:57:37.3	35.675	50.95	12.8	5.2
6	129979	2017/12/21 01:09:19.0	35.664	50.936	12	2.6
7	130486	2017/12/26 21:24:34.0	35.679	50.941	14.9	4.2
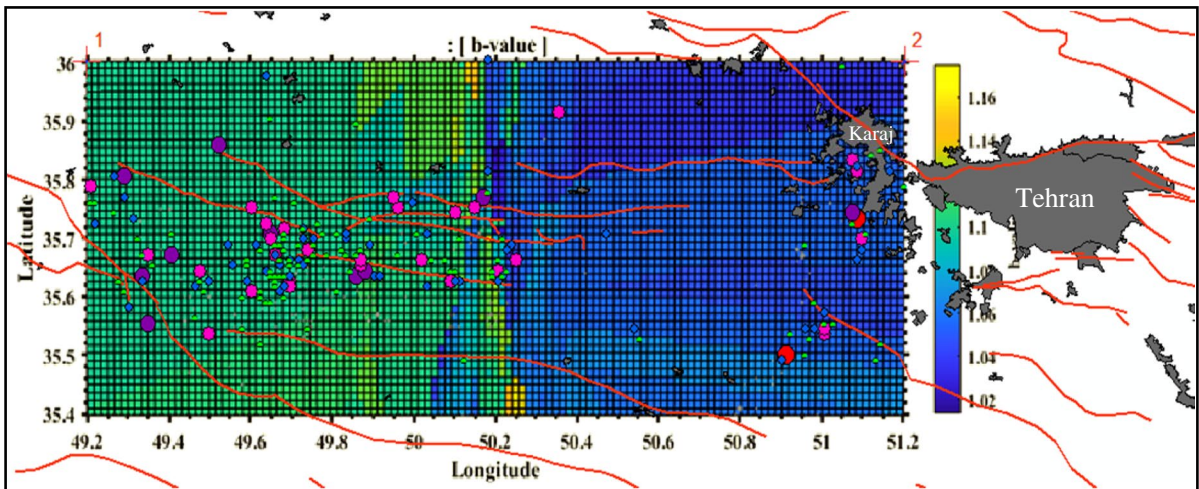
Fig. 9 The spatial variations of the *b-value* in the studied area during the period from December 2003 to January 2023

b-value for the studied area. According to this figure, local variations in this value range from approximately 1.02 to 1.16, indicating severe heterogeneity throughout the region. As mentioned earlier, the *b*-value map represents the area's stress distribution. Therefore, low *b*-values represent high stress, and high *b*-values represent low regional stress. The accumulation of stress during different periods depends on the level of asperity or creep on fault surfaces, which leads to the release of stress at different levels through either creep or earthquakes with different recurrence intervals.

As seen in Fig. 9, the *b-value* in the active fault zone of the studied area is less than 1.6. The main stress accumulation is concentrated around the Eshtehard fault. The standard deviation of the *b-value* parameter is calculated using the equation presented above (Eq. 3). According to this equation, the measured error of the *b-value* in Fig. 10 ranges from 0.1 to 0.12. This value is an acceptable standard deviation for calculating the *b-value* parameter.

The map of the *a-value* is shown in Fig. 11. This map represents lateral variations in the region's seismicity, where higher *a-values* indicate higher seismicity and lower *a-values* indicate lower seismicity. According to the figure, a varies from 4.7 to 5.1. As observed, areas with higher *a-values* have a greater concentration of earthquakes. On the other hand, areas with lower *b-values*, which indicate a lower ratio of small to large earthquakes, show a lower value due to large earthquakes. This indicates the consistency between these two maps.

4.2 Temporal distribution of b-values

We used the MLE method to calculate the temporal changes in the b values. The sample window size was 40 earthquakes. The minimum number of earthquakes
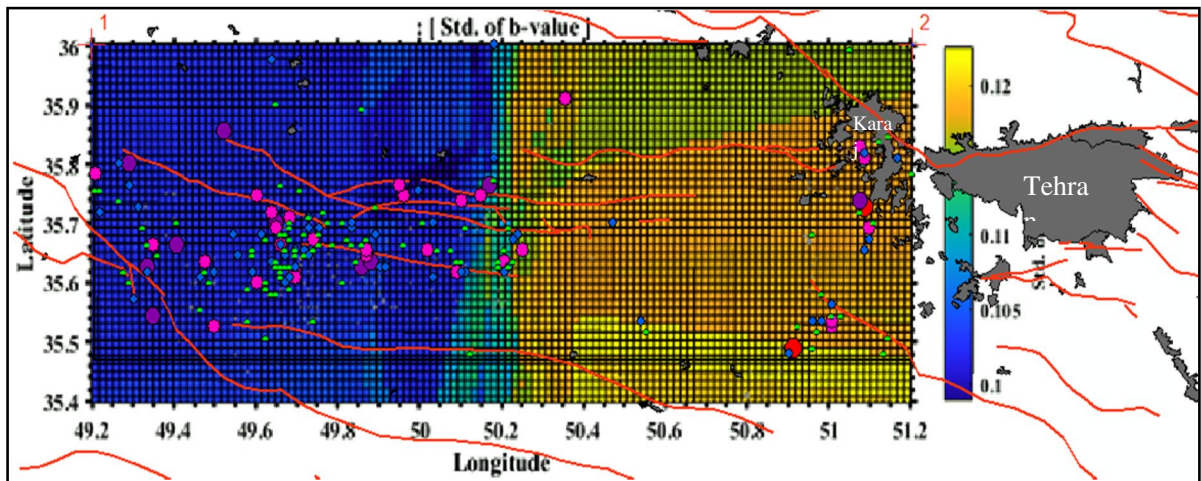
Fig. 10 The map of the standard deviation of the *b-value*
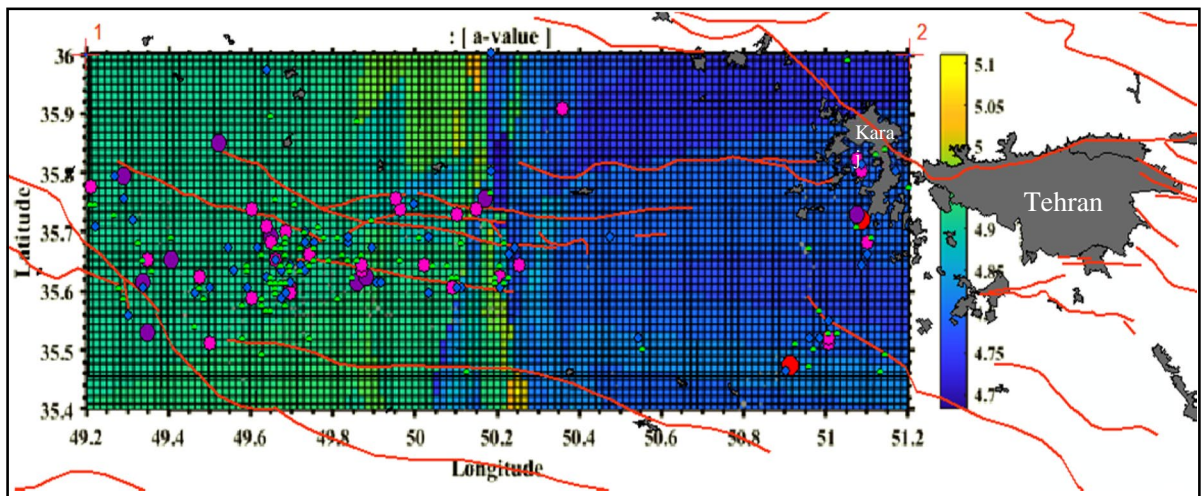
Fig. 11 The spatial variations of the *a-value* in the studied area during the period from December 2003 to January 2023

was 4, and the overlap of the windows was 4%. Figure 12 shows the decreasing trend of the b-value as a predictor of the occurrence of earthquakes with a magnitude of 4 or greater. Increasing trends in the b-value represent the number of seismic events with magnitudes equal to or less than 4 in the region. The maximum decrease in the b-value of about 1.1 was observed at the end of 2017, related to the Malard earthquake with a magnitude of 5.2 near the Eshtehard fault (Time Window 2). Another decreasing trend was observed in 2011, associated with two earthquakes in June and December (Time Window 1). At the end of these

periods, the trend has increased after a decrease, indicating a more significant accumulation of stress in the region, the possibility of earthquakes with magnitudes greater than 4, and the release of accumulated energy.

4.3 Investigating the fractal dimension in the studied area

Faults always break along the parts of their length that are irregular (Schwartz and Coppersmith 1984). The larger values of fractal dimension *D* indicate more geometric irregularities, and vice versa.

Fig. 12 The temporal variations of the *b-value* in the studied area during the period from December 2003 to January 2023
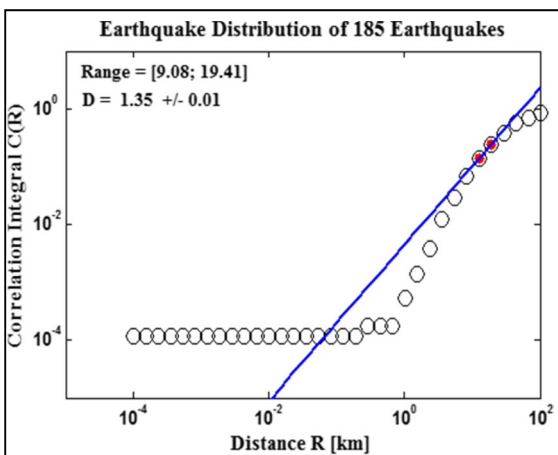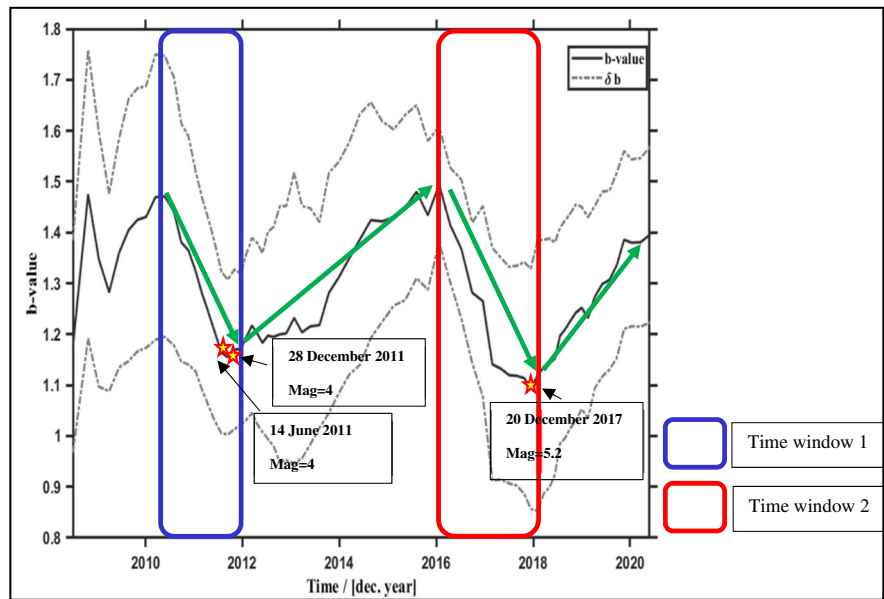
Fig. 13 Fractal value of epicenter of earthquakes for the studied area

According to theory, a set with *D = 0* represents a concentration of all events at one point, while *D = 2* represents random or homogeneous events in a two-dimensional space. Based on studies by Hirata (1989), a fractal dimension of 1.6 was obtained for Tokyo, Japan, which is an upper limit for the fractal dimension of earthquake clusters. In this study, using the correlation integral method, the fractal dimension of earthquake clusters in the studied area was calculated to be 1.35, as shown in Fig. 13.

5 Conclusion

This study's results have shown that using the frequency-magnitude distribution fractal dimension of earthquakes (through the preparation of *b-value* and *a-value* maps and fractal dimension analysis) can help us estimate and understand the seismotectonic and earthquake hazards in the region. By analyzing these parameters, we can better understand the region's seismic behavior and the potential for future seismic events, which can ultimately aid in disaster preparedness and mitigation efforts. The results of this study can be summarized as follows:

1. The *b*-value analysis over time has revealed clear variations in this parameter in late 2011 and 2017, with decreasing and increasing trends. The occurrence of earthquakes with magnitudes of 4 and 5.2 can be the reason for these changes. Overall, we have observed two decreasing trends in the studied period, which indicate the occurrence of earthquakes after a decrease in the *b-value* parameter in the region.

2. The pattern of seismic epicenter migration after the Malard earthquake with a magnitude of 5.2 shows a north–south distribution, which does not directly correlate with the Eshtehard fault's seismotectonic activity. However, since the release of stress from this block may cause stress transfer to neighboring

blocks, such as the northwestern block (North Tehran fault) in this region, it is necessary to monitor and analyze the seismic blocks around Tehran and Karaj cities by adding seismic and acceleration stations, measuring displacement vectors, and precise monitoring of fault displacements.

3. The fractal dimension of the seismic region, with an *a-value* of 1.35, indicates a moderate to strong clustering pattern of earthquakes in this area. This value also suggests that earthquakes in this region cluster together and are concentrated in specific areas. Additionally, the fractal dimension value for the seismic region indicates the geometric complexity of the clustering pattern of earthquakes in this area.

4. The destructive historical earthquake (with a magnitude of 7.2 in 1177) and the 2017 earthquake (with a magnitude of 5.2 in Malard) indicate a high earthquake hazard in the region.

5. Despite the advances that have been made in science, accurate earthquake prediction remains a difficult task. Therefore, carefully monitoring the *b-value* and seismic quiescence parameters in each area can help to better understand the seismic behavior.

Declarations

References

Aki K (1965) Maximum likelihood estimate of b in the formula log N= a-bM and its confidence limits. Bull Earthquake Res Inst Tokyo Univ 43:237–239

Allen MB, Ghassemi MR, Shahrabi M, Qorashi M (2003) Accommodation of late Cenozoic oblique shortening in the Alborz range, northern Iran. J Struct Geol 25(5):659–672

Bayrak Y, Yılmaztürk A, Öztürk S (2002) Lateral variations of the modal (a/b) values for the different regions of the world. J Geodyn 34(5):653–666

Bender B (1983) Maximum likelihood estimation of b values for magnitude grouped data. Bull Seismol Soc Am 73(3):831–851

Bengoubou-Valerius M, Gibert D (2013) Bootstrap determination of the reliability of b-values: an assessment of statistical estimators with synthetic magnitude series. Nat Hazards 65(1):443–459

Goldstein ML, Morris SA, Yen GG (2004) Problems with fitting to the power-law distribution. Eur Phys J B-Condens Matter Complex Syst 41:255–258

Grassberger P, Procaccia I (1983) Measuring the strangeness of strange attractors. Physica D 9(1–2):189–208

Gutenberg B, Richter CF (1944) Frequency of earthquakes in California. Bull Seismol Soc Am 34(4):185–188

Hirata T (1989) A correlation between the b value and the fractal dimension of earthquakes. J Geophys Res : Solid Earth 94(B6):7507–7514

Kagan YY (1993) Statistics of characteristic earthquakes. Bull Seismol Soc Am 83(1):7–24

Kagan YY, Knopoff L (1980) Spatial distribution of earthquakes: the two-point correlation function. Geophys J Int 62(2):303–320

Main I (2000) Apparent breaks in scaling in the earthquake cumulative frequency-magnitude distribution: fact or artifact? Bull Seismol Soc Am 90(1):86–97

Manakou MV, Tsapanos TM (2000) Seismicity and seismic hazard parameters evaluation in the island of Crete and the surrounding area inferred from mixed data files. Tectonophysics 321(1):157–178

Mehrnia R (2017) Geometrical fractal analysis of Malard earthquake (20 November, 2017). Environ Manag Hazards 4(4):331–345. https://doi.org/10.22059/jhsci.2018.249505.318

Miyamura S (1962) Magnitude-frequency relation of earthquakes and its bearing on geotectonics. Proc Jpn Acad 38(1):27–30

Nava FA, Márquez-Ramírez VH, Zúñiga FR, Ávila-Barrientos L, Quinteros CB (2017) Gutenberg-Richter b-value maximum likelihood estimation and sample size. J Seismolog 21:127–135

Newman ME (2005) Power laws, Pareto distributions and Zipf's law. Contemp Phys 46(5):323–351

Priestly K, Baker C, Jackson J (1994) Implications of earthquake focal mechanism data for the active tectonics of the south Caspian basin and surrounding regions. Geophys J Int 18:111–141

Rashidi A, Derakhshani R (2022) Strain and moment rates from GPS and seismological data in Northern Iran: implications for an evaluation of stress trajectories and probabilistic fault rupture hazard. Remote Sensing 14(9):2219

Schwartz DP, Coppersmith KJ (1984) Fault behavior and characteristic earthquakes: examples from the Wasatch and San Andreas fault zones. J Geophys Res : Solid Earth 89(B7):5681–5698

Shi Y, Bolt BA (1982) The standard error of the magnitude-frequency b value. Bull Seismol Soc Am 72(5):1677–1687

Utsu T (1965) A method for determining the value of b in a formula log n= a= bM showing the magnitude frequency relation for earthquakes. Geophys Bull Hokkaido Univ 13:99–103

Wiemer S (2001) A software package to analyze seismicity: ZMAP. Seismol Res Lett 72(3):373–382

Wiemer S, Wyss M (2000) Minimum magnitude of completeness in earthquake catalogs: examples from Alaska, the western United States, and Japan. Bull Seismol Soc Am 90(4):859–869

Wiemer S, Wyss M (2002) Mapping spatial variability of the frequency-magnitude distribution of earthquakes. Adv Geophys 45:259–302

Wyss M (1973) Towards a physical understanding of the earthquake frequency distribution. Geophys JR Astron Soc 31(4):341–359

Wyss M, McNutt SR, Wyss M (1998) Temporal and three-dimensional spatial analyses of the frequency–magnitude distribution near Long Valley Caldera. California Geophys J Int 134(2):409–421

Xie Z, Lyu Y, Li X (2022) Temporal and spatial changes in the b-value prior to the 2021 Luxian MS 6.0 earthquake in Sichuan China. Geomat Nat Hazards Risk 13(1):934–948

Zöller G, Hainzl S, Kurths J, Zschau J (2002) A systematic test on precursory seismic quiescence in Armenia. Nat Hazards 26:245–263